

# Adsorptive Removal of Fluoroquinolones from Water by Pectin-Functionalized Magnetic Nanoparticles: Process Optimization Using a Spectrofluorimetric Assay

Olivia A. Attallah,<sup>†</sup> Medhat A. Al-Ghobashy,<sup>‡,§</sup> Marianne Nebsen,<sup>\*,†,‡</sup> and Maissa Y. Salem<sup>‡</sup>

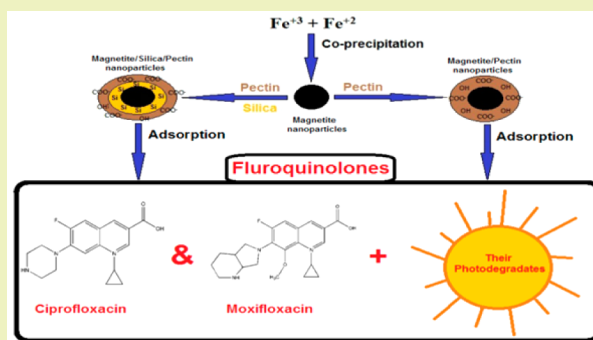
<sup>†</sup>Pharmaceutical Chemistry Department, Faculty of Pharmacy, Heliopolis University, Cairo - Belbeis Desert Road, El Salam, Cairo 11777, Egypt

<sup>‡</sup>Analytical Chemistry Department, Faculty of Pharmacy, and <sup>§</sup>Bioanalysis Research Group, Faculty of Pharmacy, Cairo University, Kasr El-Aini Street, Cairo 11562, Egypt

## S Supporting Information

**ABSTRACT:** The efficiency of adsorption of two photosensitive fluoroquinolones; Ciprofloxacin (CIP) and Moxifloxacin (MOX), on the surface of synthesized magnetite/pectin nanoparticles (MPNPs) and magnetite/silica/pectin nanoparticles (MSPNPs) was studied from aqueous solution under varying experimental conditions. A validated spectrofluorimetric assay was developed for monitoring of CIP and MOX intact drugs and their photodegraded molecules concentrations. To optimize the working conditions which influence the drugs sorption, a 2<sup>4</sup> full factorial experimental design was implemented. The maximum percentage of removal was attained as 89% (type of sorbent = MSPNPs, pH = 7.0, initial drug concentration = 5 mg/L, and contact time = 30 min). The studied factors—pH, NPs loading, initial drug concentration, and contact time—were significant for both types of sorbents. The most significant variable was pH, and the highest CIP and MOX adsorption occurred at pH = 7.0. Equilibrium isotherm data were fitted to Langmuir, Freundlich, and Sips equations, and the Sips model showed the best fit with equilibrium isotherm data. Furthermore, pseudo-first- and pseudo-second-order kinetic models were used to analyze sorption kinetics, and it was found that adsorption of the investigated fluoroquinolones followed pseudo-second-order kinetics. We believe that our synthesized NPs can be used as effective adsorbents for fluoroquinolones and their photodegraded molecules removal from aqueous solutions.

**KEYWORDS:** Pectin, magnetic nanoparticles, wastewater, ciprofloxacin, photodegradates, factorial design



## INTRODUCTION

Drugs used in both human and veterinary medicine have been detected in surface water and groundwater in concentrations ranging from ng/L to mg/L.<sup>1</sup> Among these drugs are antibiotics and their metabolites which can reach the environment through different ways, such as pharmaceutical manufacturing plants effluents, human or animal wastes, hospital wastewater, and municipal wastewater treatment plants.<sup>2</sup> One group of antibiotics receiving considerable attention is the fluoroquinolones (FQs).<sup>3</sup> FQ antibiotics are the fourth most used medicines for human beings, and they are useful in treatment of infections after intra-ocular procedures such as cataract, glaucoma, and corneal surgery.<sup>4</sup> Studies reported also that FQ antibiotics may be genotoxic.<sup>5</sup> In addition, FQs are incompletely metabolized inside the human body. 20%–80% of them are excreted in their pharmacologically active forms; thus, they can cause antibiotic resistance in certain bacteria.<sup>2,6</sup> Several studies have revealed an increase of the concentration of FQs in the aquatic environment, up to levels of  $\mu\text{g/L}$ .<sup>7,8</sup> Consequently, the presence of FQ pollutants in the environment threatens the safety of drinking

water and aquatic ecosystems, and they must be either removed from water or degraded. The elimination of FQs from drinking water and wastewater by direct photolysis,<sup>9</sup> advanced oxidation processes (AOPs),<sup>10</sup> and adsorption<sup>11</sup> has been reported.

Photolysis using direct sunlight is one of the most economic techniques for removal of FQs. However, individual FQs can undergo spontaneous photolysis to different degrees, depending on their chemical structure.<sup>12</sup> A drawback of direct photolysis is the incomplete conversion of FQs into pharmacologically inactive moieties, which limits the use of such a technique.<sup>3,12</sup> AOPs show a potential to degrade soluble antibiotics effectively via formation of reactive hydroxyl radical ( $\bullet\text{OH}$ ) species.<sup>6</sup> Nevertheless, the cost of AOPs is fairly high, and some techniques require pretreatment of wastewater to ensure reliable performance.<sup>13</sup>

One of the most studied techniques nowadays for wastewater treatment is adsorption. The popularity of such a technique is

Received: May 9, 2016

Revised: November 17, 2016

Published: December 13, 2016

elaborated from the ability to remove pollutants that are too stable for other methods and the use of low-cost materials, which in turn reduces the overall treatment cost.<sup>14</sup> Generally, the adsorption process is affected by many factors, such as the adsorbent's surface area, the adsorbent/adsorbate interaction, pH, contact time, and temperature.<sup>14</sup> The adsorption technique has been applied for the removal of FQs from wastewater in several studies. Xing et al.<sup>11</sup> investigated the efficiency of ciprofloxacin adsorption on synthesized birnessite under varying physicochemical conditions, such as solution pH, contact time, initial ciprofloxacin concentration, and different average oxidation states of Mn in birnessite.

Yao et al.<sup>4</sup> studied the adsorption of FQs using sludge-derived biochar made of various wastewater sludges. High adsorption capacity of sludge-derived biochar was observed with adsorption capacity up to 19.80 mg/g. The emergence of tailored nanoparticles with magnetic properties and high adsorption competence for a mixture of compounds offers a novel tool to deal with wastewater purification.<sup>15,16</sup> In recent years, magnetic nanoparticles (MNPs) have been successfully implemented to remove or extract FQs. For instance, Wei et al.<sup>6</sup> used Fe<sub>3</sub>O<sub>4</sub> magnetic nanoparticles as a peroxidase mimetic to accelerate levofloxacin sonodegradation in an ultrasound (US)/H<sub>2</sub>O<sub>2</sub> system. In addition, Huang et al.<sup>17</sup> used poly(vinylimidazole-co-divinylbenzene) magnetic nanoparticles for the adsorption of FQs from environmental water samples. Ding et al.<sup>18</sup> also used ciprofloxacin as a template molecule to prepare a magnetic molecularly imprinted polymer that is selective to FQs. On the other hand, He et al.<sup>19</sup> developed a new technique for the isolation of FQs from egg samples by molecularly imprinted polymers on the surface of magnetic carbon nanotubes using ofloxacin as a pseudotemplate.

Noticeably, the adsorption efficiency of magnetic nanoparticles depends on the type of NPs surface modification. Such modified surfaces can provide functional groups to MNPs for interaction with various types of compounds.<sup>20</sup> Hybrid nanomaterials of polysaccharide—pectin and magnetite nanoparticles—have been reported.<sup>21</sup> Pectin is a valuable byproduct that is most commonly obtained from wastes of fruits such as pomelo peel, citrus peel, banana peel, passion fruit rind, and nutmeg rind.<sup>22,23</sup> The adsorptive removal of FQs and their degradation products from aqueous solutions using hybrids of

pectin and magnetic nanoparticles has not been previously reported. Adsorption should provide a novel approach for removal of FQs along with their closely related photolysis product, that might be formed spontaneously or via metabolites.

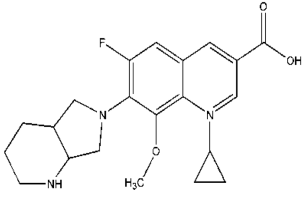
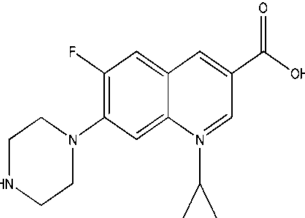
Several analytical methodologies have been reported for determination of FQs and their degradation products in aqueous solutions including HPLC,<sup>3</sup> spectrofluorimetry,<sup>24</sup> spectroscopy,<sup>25</sup> polarography,<sup>26</sup> voltammetry,<sup>27</sup> and capillary electrophoresis.<sup>28</sup> In particular, spectrofluorimetry as an analytical technique is being utilized with increasing frequency in a wide variety of research fields from medicine to physics.<sup>29</sup> The main advantage of spectrofluorimetry over HPLC methods is the speediness of execution as the measurements of fluorescence are instantaneous. Spectrofluorimetry can also improve the limit of detection and possesses good analytical selectivity and higher capacity against blank interference when compared with other spectrophotometric methods.<sup>24</sup> Moreover, it can be used to evaluate the adsorption capacity of the synthesized particles toward not only intact FQs but also their photolysis products and/or metabolites that retain the same fluorophore.

Our aim in this work was to remove fluoroquinolones and their photodegraded molecules that are readily formed in aqueous solution upon exposure to light using the adsorptive power of two pectin magnetic nanohybrids as an approach to water treatment. Full factorial design (2<sup>4</sup>) was used to evaluate the relative significance of four experimental factors concerning the adsorption quantities of two model fluoroquinolones (FQs)—Moxifloxacin (MOX) and Ciprofloxacin (CIP) (structures are shown in Table 1)—on the surfaces of pectin modified magnetic nanoparticles: magnetite/pectin NPs (MPNPs) and magnetite/silica/pectin NPs (MSPNPs). The isotherms and kinetics of adsorption of the model FQs were also calculated. A validated spectrofluorimetric assay has been developed for monitoring the model FQs throughout the treatment process. The proposed adsorbents (MSPNPs and MPNPs) were targeted to remove not only the intact molecules but also their photodegraded molecules that were naturally present as well as their metabolites.

## EXPERIMENTAL SECTION

**Instrumentation.** A Cary Eclipse Fluorescence spectrophotometer model FLR-S/W (G9550-64000) (Agilent Technologies, USA) was

Table 1. Model Fluoroquinolones in the Present Study<sup>30,31</sup>

Drug	IUPAC name	Structure	Physical characters			
			Mwt	Log P	pKa	H <sub>2</sub> O solubility
Moxifloxacin (MOX)	1-Cyclopropyl-6-fluoro-7-((4aS,7aS)-hexahydro-1H-pyrrolo[3,4-b]pyridin-6(2H)-yl)-8-methoxy-4-oxo-1,4-dihydroquinoline-3-carboxylic acid		401.43	2.9	5.69, 9.42	0.168 mg/mL
Ciprofloxacin (CIP)	1-cyclopropyl-6-fluoro-4-oxo-7-(piperazin-1-yl)-1,4-dihydroquinoline-3-carboxylic acid		331.34	0.28	6.09	1.35 mg/mL

used for drugs concentration analysis. FQs samples photodegradation was confirmed using an HPLC system model 1100 (Agilent Technologies, USA) with a variable wavelength detector. The system was controlled using Chemstation software.

**Materials.** Ferric chloride anhydrous ( $\text{FeCl}_3$ ), ferrous sulfate ( $\text{FeSO}_4 \cdot 7\text{H}_2\text{O}$ ), pectin from the rind of citrus or apple (Galacturonic acid  $\geq 74.0\%$ ), and tetraethoxysilane (TEOS) were purchased from Fisher Scientific (USA). Moxifloxacin and Ciprofloxacin were supplied from Bayer, Egypt. HPLC grade acetonitrile was purchased from Fisher Scientific (UK). Ammonium acetate was purchased from Sigma-Aldrich (Germany). All other chemicals and reagents used were of analytical grade or higher. Deionized water was obtained using a Milli-Q UF-Plus system (Millipore, Eschborn, Germany).

**Synthesis of pectin modified magnetite nanoparticles, magnetite/pectin nanoparticles (MPNPs), and magnetite/silica/pectin nanoparticles (MSPNPs).** The synthesis and characterization of core-shell MPNPs and MSPNPs was performed according to our previous work.<sup>32</sup> Fabrication of the core-shell MPNPs involved the preparation of (0.5% W/V) pectin solution by dissolving the corresponding mass in 250 mL of deionized water. Continuous stirring of the prepared solution was done for 24 h at room temperature. An aliquot of 50 mL of solution of ferrous and ferric ions (molar ratio = 1:2) was added dropwise to the pectin solution under vigorous stirring. Magnetite formation was observed after dropwise addition of ammonia (33% W/W) to the prepared solution. Stirring was continued for another 30 min, and the black precipitate was then washed with distilled water and dried in the oven at 90 °C.<sup>32</sup>

Synthesis of the double shell MSPNPs was performed by dissolving  $\text{FeSO}_4 \cdot 7\text{H}_2\text{O}$  and  $\text{FeCl}_3$  (molar ratio, 1:2) in 20 mL of deionized water and stirring for 20 min. Dropwise addition of 30 g% NaOH solution with vigorous stirring was carried out until a black precipitate of magnetite nanoparticles was formed. The nanoparticles were then separated and washed with water. A suspension of the prepared magnetite nanoparticles ( $\approx 1.00$  g) was diluted with a mixture of deionized water (18.5 mL) and ethanol (80 mL). Addition of ammonia solution (0.5 mL, 33% W/W) and TEOS (1 mL) to the mixture solution was performed under mechanical stirring for 16 h. The formed magnetite/silica NPs were washed with deionized water and ethanol. Pectin solution of 0.5 W/V% was prepared and added dropwise to a 25 mL suspension of the magnetite/silica NPs ( $\approx 1.00$  g) and stirred for 24 h. The product was then collected by magnetic decantation, washed with deionized water, and dried in the oven at 60 °C.

The synthesized MPNPs had a spherical shape (200–500 nm in diameter) while the MSPNPs were smaller in size with an average diameter of  $25 \pm 5$  nm. The magnetic behavior of the MSPNPs and MPNPs was recorded with magnetic saturation of 29.2 and 34.9 emu/g, respectively. In addition, the pH of zero point charge of MSPNPs and MPNPs was recorded as 2.5 and 2.2, respectively.<sup>32</sup>

**Photodegradation of the model FQs.** Direct photolysis of CIP and MOX drugs was achieved by exposing solutions of the intact drugs (10  $\mu\text{g}/\text{mL}$ ) to direct sunlight for 6 h to simulate real aquatic environments.<sup>2</sup> The intact and photodegraded samples of CIP and MOX were checked by spectrofluorimetric and HPLC assays. The HPLC assay was performed at room temperature using a ZORBAX Eclipse XDB-C18 column (250  $\times$  4.6 mm, 5  $\mu\text{m}$ ). The mobile phase constituted a system of acetonitrile and 10 mM ammonium acetate buffer, pH 3.5 (70:30). Detection was carried out at 280 nm, flow rate was adjusted at 1 mL/min, and the injection volume was 20  $\mu\text{L}$ .

**Spectrofluorimetric analysis method.** Solutions of both intact drugs and photodegraded samples (1  $\mu\text{g}/\text{mL}$ ) were scanned in the range 200–600 nm, and the wavelengths of excitation and emission for each drug and their photodegraded molecules were determined. Standard solutions of each CIP and MOX (5 mg/L) were prepared in deionized water. Accurate volumes of CIP and MOX stock solutions were transferred separately into a set of 25 mL volumetric flasks and diluted to volume with phosphate buffer (pH 7.0). Calibration curves for both drugs were obtained by plotting fluorescence intensity at the wavelength of emission ( $\lambda_{\text{em}}$ ) of each drug against concentration.

**Evaluation of adsorption efficiency.** *Initial studies.* Studies were performed on FQs (CIP and MOX) photodegraded samples to evaluate

the capability of the MSP and MPNPs to adsorb the model FQs and their photodegraded molecules from aqueous solution and to determine the contact time necessary to reach equilibrium. 0.5  $\mu\text{g}/\text{mL}$  of MSPNPs and MPNPs was added to 25 mL of the CIP and MOX photodegraded sample solutions of 10 mg/L initial concentration at natural pH and agitated with a speed of 200 rpm at 25 °C. Experiments were repeated, and the fluorescence of drugs together with their photodegraded molecules left in the supernatant solutions after separation was determined at defined time intervals.

*Experimental design.* Full  $2^4$  factorial design was used to understand the relative significance and interactions of the initial FQs concentration, loading of NPs, pH, and contact time on the amount of drug adsorbed. Table 2 summarizes the studied factors and their corresponding levels.

**Table 2. Actual Factors and Their Levels Used for Two-Level Full Factorial Design Experiment**

Factor name	Factor code	Low level (-1)	High level (+1)
NPs loading ( $\mu\text{g}/\text{mL}$ )	A	0.5	1.0
Initial drug concentration (mg/L)	B	5.0	10.0
pH	C	3.0	7.0
Contact time (min)	D	15.0	30.0

The adsorptions of the model FQs (CIP and MOX) and their photodegraded molecules were performed by shaking 25 mL of each of the photodegraded drugs solutions separately at 200 rpm at 25 °C under conditions as specified in each experiment (Tables 4 and 5). The pH values of the solutions were adjusted using 0.1 M NaOH and/or 0.1 M HCl solutions. After a predetermined contact time, supernatants were separated and suitably diluted, and the concentrations of the drugs along with their photodegraded molecules were determined spectrofluorimetrically. Results were evaluated in comparison to those obtained from a photodegraded control sample that has not been subjected to both types of NPs. Statistical calculations (analysis of variance (ANOVA), *F*-tests, normality test, and regression analysis) were implemented using Minitab. Error functions such as  $R^2$  test were performed to find out the proper kinetic models to represent the studied adsorption experiments.

*Adsorption isotherms.* Equilibrium study was performed by shaking solutions of different initial model FQs concentrations (5 and 25 mg/L) separately with 1  $\mu\text{g}/\text{mL}$  of both types of adsorbents (MSPNPs and MPNPs) for 30 min at pH 7.0. After equilibrium, the amount of drug adsorbed ( $q_e$ , mg/g) was determined and plotted against the equilibrium concentration ( $C_e$ , mg/mL).

*Kinetics of adsorption.* Kinetic study experiments were conducted using 10 mg/L model FQs photodegraded solutions. Experimental FQs solutions were shaken with 0.5  $\mu\text{g}/\text{mL}$  of MSPNPs and MPNPs at pH 7.0 for different time intervals (15–60 min). The concentration of drugs and their photodegraded molecules in solutions was determined, and the amount of drug adsorbed at each time interval ( $q_t$ , mg/g) was plotted against time ( $t$ , min).

*Data analysis.* The amounts of drug adsorbed at time  $t$  ( $q_t$ ) and at equilibrium ( $q_e$ ) were calculated using the mass balance equation  $q_t = (C_0 - C_t) (V/m)$ , where  $C_0$  and  $C_t$  (mg/L) are the initial and final drug concentrations, respectively,  $V$  (L) is the volume of the drug solution, and  $m$  (g) is the mass of adsorbent. When  $t$  equals the equilibrium time, then  $C_t = C_e$ ,  $q_t = q_e$ , and  $q_e$  can be calculated from the above equation. Furthermore, the amount of drugs removed is generally expressed in percentage ( $R$ , %) and calculated using the equation  $R = 100(C_0 - C_e)/C_0$ .

## RESULTS AND DISCUSSION

In this study, pectin modified magnetic NPs—MPNPs and MSPNPs—were investigated for their capability to remove FQs and their photodegraded molecules from aqueous solutions. A  $2^4$  factorial design was implemented, and the studied factors (NPs loading, drug concentration, pH, and contact time) and their levels were chosen accurately to reach the best optimization

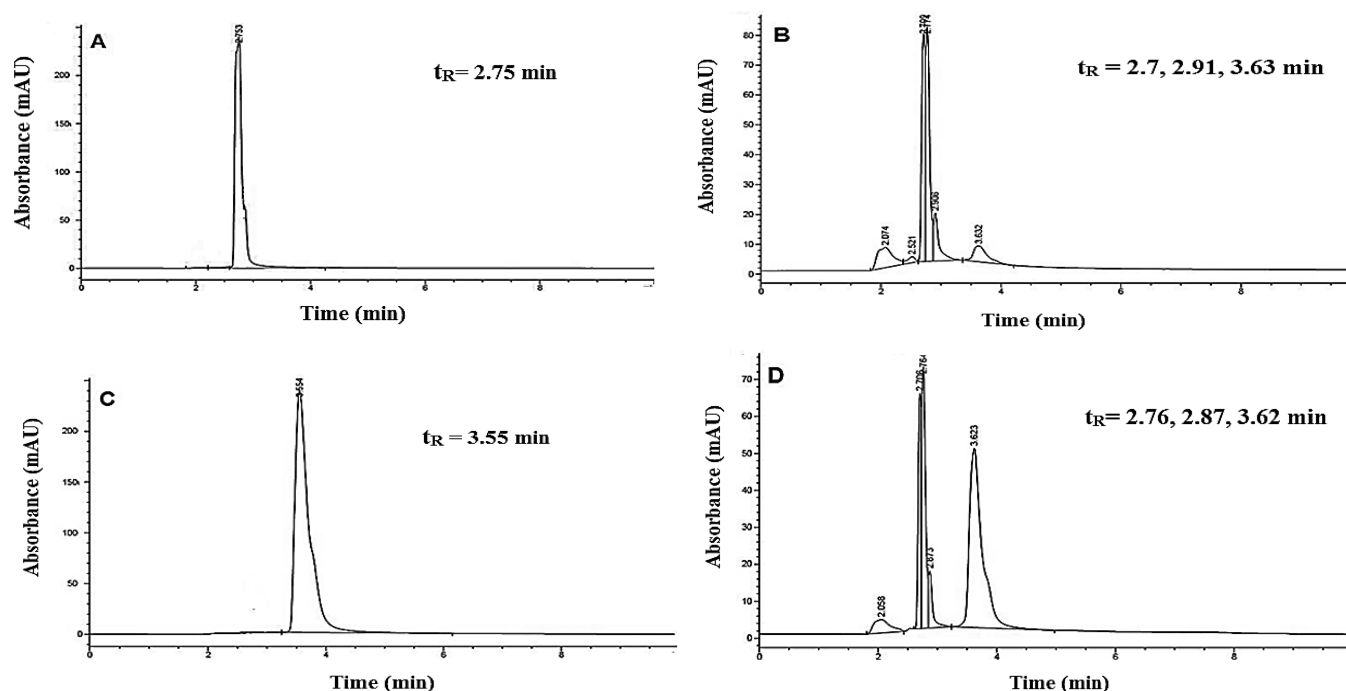


Figure 1. HPLC chromatograms of (A) CIP drug, (B) partially degraded samples of CIP, (C) MOX drug, and (D) partially degraded samples of MOX.

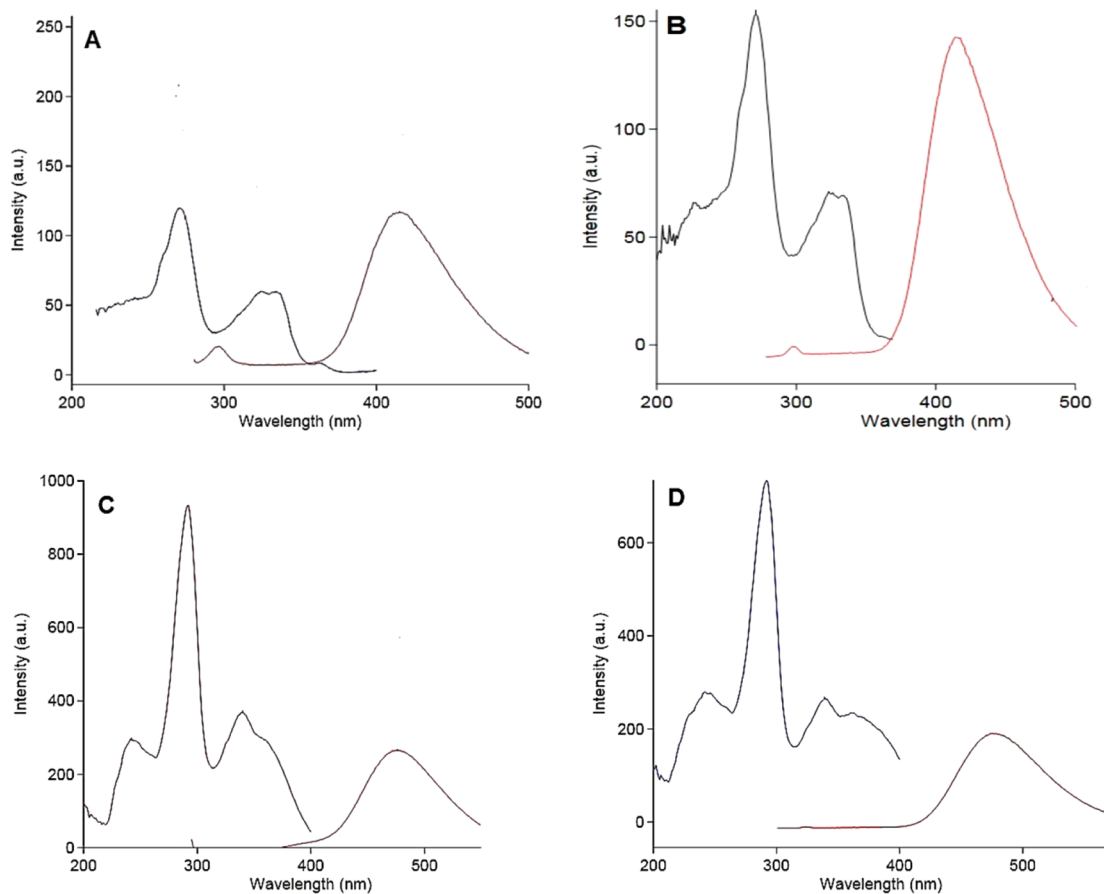


Figure 2. Spectrofluorimetric curves of (A) CIP drug, (B) partially degraded samples of CIP, (C) MOX drug, and (D) partially degraded samples of MOX.

of the adsorption process. The studied levels for the pH factor were (pH = 3 and 7); at such pH values the FQs are found in the cationic and zwitterionic forms, respectively.<sup>11</sup> According to

previous literature, it was found that the optimum pH for adsorption was pH 6–7, where the FQs are in their zwitterionic form with some cationic amine groups.<sup>11,17</sup> Regarding the FQs

concentrations, low concentrations were chosen (5–10  $\mu\text{g}/\text{mL}$ ) in order to mimic the concentration of FQs in real environmental waste samples.<sup>36</sup> For the factor of contact time, the selected values for the low and high levels were 15 and 30 min, the time taken in the preliminary experiments to reach equilibrium.

**Photodegradation of FQs.** HPLC analysis was done to confirm the photodegradation of the intact drugs (CIP and MOX) and formation of their photodegraded molecules. Figure 1 demonstrates the chromatograms of the intact drugs and their partially degraded samples. We can observe the presence of single peaks of the intact drugs in Figure 1A and C for CIP ( $t_R = 2.75$  min) and MOX (3.55 min), respectively. Figure 1B and D illustrate the occurrence of partial degradation of the intact drugs, CIP and MOX, respectively, with the appearance of additional peaks at  $t_R = 2.7$ , 2.91, and 3.63 min for CIP and a forked prominent peak at 2.76 and 2.87 min. The clear differences between the chromatograms of the intact drugs and the photodegraded samples confirm the formation of degradation products in both drugs.

**Spectrofluorimetric analysis method.** Analysis of the photodegraded samples of the model FQs was carried out using a spectrofluorimetric assay. Figure 2 shows the excitation and emission spectra of the intact drugs and their photodegraded samples. The wavelengths of maximum excitation ( $\lambda_{ex}$ ) and emission ( $\lambda_{em}$ ) for CIP and its photodegraded molecules were 270 and 415 nm, respectively, while MOX and its photodegraded molecules showed a wavelength of maximum excitation and emission at 292 and 475 nm, respectively. Such results indicated that the photodegraded molecules of the drugs have similar fluorescence characteristics as their intact drugs because they contain the same fluorophore (quinolone ring).<sup>3</sup> To assess the efficiency of quantitation of the intact drugs and their photodegraded forms using the spectrofluorimetric assay, mixtures of the intact drugs and their photodegraded samples were analyzed and the fluorescence intensity was determined. It was found that, upon addition of equal proportions of the intact drug and its photodegraded sample, the fluorescence intensity increased proportionally (results not shown). Consequently, a calibration curve was constructed for each drug using the standards of intact drugs. Method validation was done according to ICH Q2B guidelines for validation of analytical assays with respect to linearity, accuracy, precision (within and between days), limit of detection (LOD), and limit of quantification (LOQ).<sup>33–35</sup>

Table 3 shows a summary for validation results. The plots showed good linearity with small intercepts and good correlation coefficients ranging from 0.9996 to 0.9998.

**Evaluation of adsorption efficiency. Initial studies.** The adsorption efficiency of MSPNPs and MPNPs (0.5  $\mu\text{g}/\text{mL}$ , each) was demonstrated using CIP and MOX control samples (10 mg/L, natural pH). Such a small concentration was chosen to somehow simulate the concentrations of FQs in real wastewater samples (ng/L to  $\mu\text{g}/\text{L}$ ).<sup>36</sup> The effect of contact time on the adsorption of CIP and MOX together with their photodegraded molecules was also studied to determine the time required by aliquots of 0.5  $\mu\text{g}/\text{mL}$  MSPNPs and MPNPs to adsorb 10 mg/L of the model FQs from solution at natural pH. MSPNPs and MPNPs efficiencies of removal of CIP and MOX are shown in Figure 3 (a) and (b), respectively. Within the first 15 min, there was a significant increase in the percentage of drugs removal. Upon increasing the contact time, a slow increase in the removal percentage was observed. After 30 min, the MSPNPs showed an efficiency of removal reaching 73.02% and 65.67% for CIP and MOX, respectively. On the other hand, the MPNPs had

**Table 3. Spectrofluorimetric Method Validation for Determination of Model Fluoroquinolones (MOX and CIP)**

Item	MOX	CIP
Wavelength of excitation	287 nm	270 nm
Wavelength of emission	465 nm	415 nm
Range of linearity	100–1200 ng/mL	100–1200 ng/mL
Regression equation	Fl intensity = 0.241 $C_{\text{ng/mL}}$ + 5.5433	Fl intensity = 0.3288 $C_{\text{ng/mL}}$ + 7.4437
Regression coefficient ( $r^2$ )	0.9995	0.9998
LOD ( $\text{ng mL}^{-1}$ )	31.92	21.58
LOQ ( $\text{ng mL}^{-1}$ )	96.73	65.39
$S_b$ (SD of slope)	1.695	1.564
$S_a$ (SD of intercept)	0.0026	0.0024
Accuracy Mean $\pm$ S.D.	100.66 $\pm$ 1.08	101.03 $\pm$ 1.09
Repeatability (%RSD, $n = 6$ )	0.395	1.497
Precision		
Intraday %RSD ( $n = 3$ )	0.17–0.52	0.19–0.26
Interday %RSD ( $n = 3$ )	0.42–1.61	2.27–2.47

a removal efficiency of 53.38% and 61.21% for CIP and MOX, respectively. The adsorption of drugs on the NPs reached equilibrium after 15–30 min even after extending the experimental time to 60 min.

**Experimental design.** Additional investigations were performed to optimize the studied effects of (A) MP and MSPNPs, (B) initial FQs concentration, (C) pH, and (D) contact time on the efficiency of FQs adsorption. Such factors were chosen based upon previously reported studies in the literature.<sup>37–39</sup> Full factorial design was employed to evaluate the interactions between the studied factors, and each factor level of significance, in addition to the optimum experimental conditions necessary to optimize the process of model FQs adsorption (Table 1). Analysis of samples was done using a spectrofluorimetric assay, and percentage of FQs removal was calculated (Table 4 and Table 5 for MSPNPs and MPNPs, respectively).

**Statistical analysis.** The 95% confidence level was used to analyze the full factorial design results, and the percentage of removal was taken as the response factor. The relative significance of the studied factors and the interactions between them were determined from the Pareto diagram. The direction of effects is obtained from the normal plot of the standardized effects. Within the studied range, a positive effect indicates an increase in the studied response at high levels of the respective variables, while a negative effect indicates an increase in the response at low levels of these variables.<sup>40</sup>

In this study, pH (C), NPs loading (A), and contact time (D) were found of significant impact with a positive effect while initial FQs concentration (B) was significant but with a negative effect for both types of NPs (Figure 4 and Figure 5 for MSPNPs and MPNPs, respectively).

The interaction effects were estimated through the analysis of variance (ANOVA). The ANOVA results for CIP and MOX adsorption together with their photodegraded molecules on MSPNPs are shown in Table S2-S1 and Table S3-S2, respectively, while the ANOVA results for CIP and MOX adsorption together with their photodegraded molecules on MPNPs are demonstrated in Table S4-S3 and Table S5-S4, respectively.

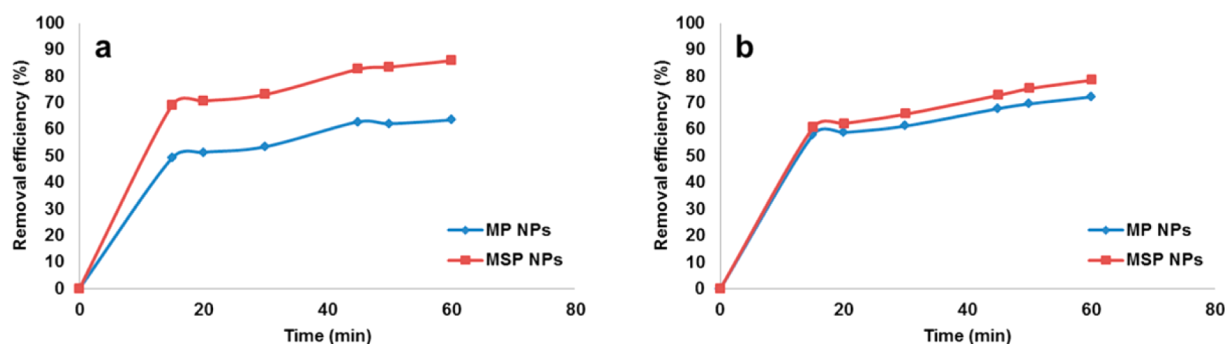


**Figure 3.** Effect of contact time on the removal efficiency of (a) CIP drug and its degradation products and (b) MOX drug and its degradation products. Adsorbent: 0.5  $\mu\text{g/mL}$ , drug: 10 mg/L, temperature: 25  $^{\circ}\text{C}$ , pH: natural pH of drugs, time: 60 min.

**Table 4.** Design Matrix for  $2^4$  for Full Factorial Design Employed for the Model Fluoroquinolones Removal by MSPNPs and Results Obtained Using the Spectrofluorimetric Assay

Run No.	Factor Code				Spectrofluorimetry			Spectrofluorimetry		
					MOX conc. (mg/L)	%Removal		CIP conc. (mg/L)	%Removal	
	A	B	C	D		Exp <sup>a</sup>	Cal <sup>b</sup>		Exp <sup>a</sup>	Cal <sup>b</sup>
1	+1	-1	+1	+1	0.52	89.56	91.42	0.54	89.28	89.84
2	-1	-1	-1	+1	3.33	33.35	31.76	3.46	30.80	30.12
3	0	0	0	0	3.32	55.70	53.60	3.33	55.57	53.82
4	-1	+1	-1	-1	8.06	19.41	17.39	8.14	18.64	17.81
5	+1	+1	+1	-1	2.50	74.95	76.38	2.15	78.53	78.95
6	+1	-1	+1	-1	0.73	85.48	83.88	0.67	86.67	86.33
7	-1	+1	-1	+1	7.86	21.36	23.65	7.96	20.35	21.39
8	+1	-1	-1	-1	3.11	37.72	37.05	3.42	31.67	31.33
9	-1	-1	-1	-1	3.84	23.24	25.10	3.71	25.86	26.77
10	+1	-1	-1	+1	2.79	44.08	45.02	3.29	34.05	34.61
11	-1	+1	+1	-1	3.94	60.61	60.36	3.09	69.13	69.27
12	-1	-1	+1	+1	0.89	82.18	81.50	0.76	84.77	84.77
13	+1	+1	-1	-1	7.56	24.42	25.79	7.60	23.98	24.68
14	+1	+1	-1	+1	6.55	34.47	33.36	7.13	28.68	28.20
15	-1	-1	+1	-1	1.28	74.34	75.28	0.95	80.97	81.19
16	-1	+1	+1	+1	3.43	65.67	66.18	2.69	73.02	73.09
17	+1	+1	+1	+1	1.53	84.68	83.51	1.71	82.90	82.70

<sup>a</sup>Calculated relative to the results of an equivalent control sample that has not been subjected to MSPNPs. <sup>b</sup>Theoretically calculated by Minitab software using the regression model.

Based upon the ANOVA calculations of Fisher's F-ratios, P-values, and factors effects, it was predicted that the main factors—pH, NPs loading, initial FQs concentration, and contact time—were of high significance ( $P < 0.05$ ).

Although the main effects gave a clear idea, the interaction effects of the significant factors (contact time, NPs loading, pH, and initial drug concentration) were also graphically demonstrated in Figure S6-S1 and Figure S7-S2 for MSPNPs and MPNPs, respectively, to give a better insight of the process.

Noticeably, parallel lines indicate no interaction while non-parallel lines suggest that an interaction occurs, and the more non-parallel the lines are, the greater the strength of the interaction. In most of our interaction plots, (Figure S6-S1 and Figure S7-S2), the lines are parallel. This indicates that no interaction occurs between our main effects, and such results come in accordance with that of an ANOVA test where the P-values of the interaction effects are  $>0.05$ .

**Normal probability analysis.** The graphical plot of normal probability is generally used to determine whether the data is distributed normally or not.<sup>41</sup> The data is distributed normally if all the points fall close to the straight line.<sup>38</sup> The normal probability plots of residual values of CIP and MOX are shown in

Figure 6(a) and Figure 6(b), respectively, when MSPNPs are used as adsorbent, while Figure 7(a) and Figure 7(b) show the normal probability plots of residual values of CIP and MOX, respectively, while using MPNPs as adsorbent. The P-values ( $P > 0.05$ ) indicate that the experimental points were normally distributed. The regression equation summarizing the experimental design is given in Table 6 together with the regression coefficients and P-values.

**Mechanism of adsorption.** pH played an important role in the removal of the model FQs together with their photodegraded molecules from aqueous solution. The extent of CIP and MOX adsorption onto the surface of NPs is mainly affected by the type of charge on the surface, which, in turn, is influenced by the pH of the solution. The results showed that the maximum adsorption of MOX and CIP was noted at pH 7.0. At such pH, the MP and MSPNPs surfaces turned out to be negatively charged while the MOX and CIP were in their zwitterionic form. Even though the net charge of the drugs' molecules was zero, the protonated amine group was still able to contribute to the adsorption of MOX and CIP on both types of NPs. However, when the solution pH was 3.0, the adsorption was lower. This could be attributed to the decrease in the negative charge on the NPs

**Table 5. Design Matrix for 2<sup>4</sup> for Full Factorial Design Employed for the Model Fluoroquinolones Removal by MPNPs and Results Obtained Using the Spectrofluorimetric Assay**

Run No.	Factor Code				Spectrofluorimetry			Spectrofluorimetry		
					MOX conc. (mg/L)	%Removal		CIP conc. (mg/L)	%Removal	
	A	B	C	D		Exp <sup>a</sup>	Cal <sup>b</sup>		Exp <sup>a</sup>	Cal <sup>b</sup>
1	+1	-1	+1	+1	0.63	87.32	88.53	1.29	74.28	76.61
2	-1	-1	-1	+1	3.39	32.29	31.14	3.55	29.08	29.40
3	0	0	0	0	3.43	54.23	48.69	3.92	47.8	45.20
4	-1	+1	-1	-1	8.28	17.18	16.81	8.51	14.91	14.43
5	+1	+1	+1	-1	3.48	61.50	63.48	3.67	63.28	64.81
6	+1	-1	+1	-1	1.08	78.32	77.31	1.36	72.78	70.77
7	-1	+1	-1	+1	8.05	19.46	20.02	7.92	20.85	21.64
8	+1	-1	-1	-1	3.36	32.76	32.27	3.25	34.93	30.61
9	-1	-1	-1	-1	3.89	22.01	23.36	3.73	25.32	30.61
10	+1	-1	-1	+1	2.99	40.28	40.97	3.07	38.70	38.06
11	-1	+1	+1	-1	4.21	57.93	56.79	5.08	49.22	48.66
12	-1	-1	+1	+1	1.32	73.52	73.16	1.45	70.96	69.60
13	+1	+1	-1	-1	7.21	27.93	27.83	7.69	23.00	23.15
14	+1	+1	-1	+1	6.83	31.66	31.95	7.11	28.87	29.05
15	-1	-1	+1	-1	1.89	62.31	62.85	1.96	60.77	62.45
16	-1	+1	+1	+1	3.88	61.20	62.52	4.66	53.37	54.26
17	+1	+1	+1	+1	2.81	71.92	70.12	2.97	70.33	69.12

<sup>a</sup>Calculated relative to the results of an equivalent control sample that has not been subjected to MPNPs. <sup>b</sup>Theoretically calculated by Minitab software using the regression model.

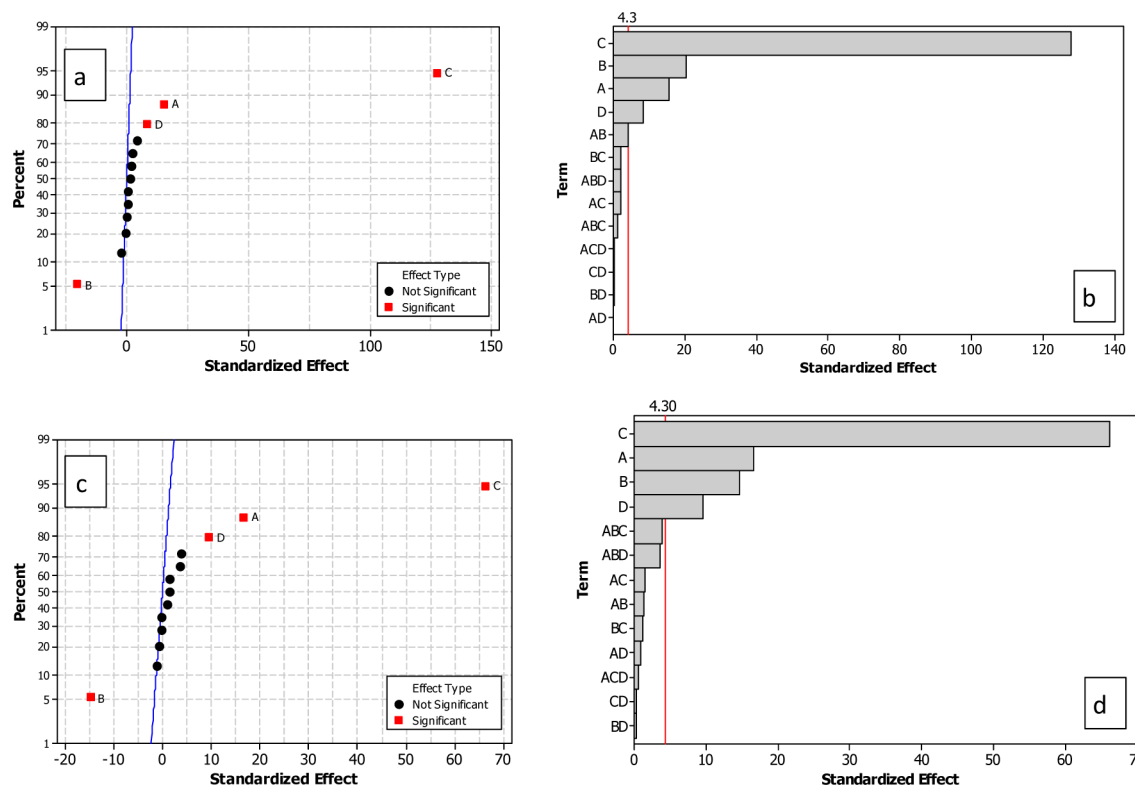


**Figure 4.** (a) Normal plot of the standardized effect of single and interaction factors on % CIP removal by MSPNPs. (b) Pareto chart of the standardized effects of single and interaction factors on % CIP removal by MSPNPs. (c) Normal plot of the standardized effect of single and interaction factors on % MOX removal by MSPNPs. (d) Pareto chart of the standardized effects of single and interaction factors on % MOX removal by MSPNPs. (A = NPs loading, B = Drug concentration, C = pH, and D = contact time).

surface at low pH leading to repulsion with the positively charged CIP and MOX. Such results are in agreement with that of the literature.<sup>11,17</sup> It should be noted also that MSPNPs showed better removal efficiency for CIP and MOX than MPNPs due to

the presence of the additional negatively charged silica layer to the pectin layer on the surface of MSPNPs.

**Adsorption isotherms.** Different initial concentrations of model FQs (5–25 mg/L) were used to study the equilibrium

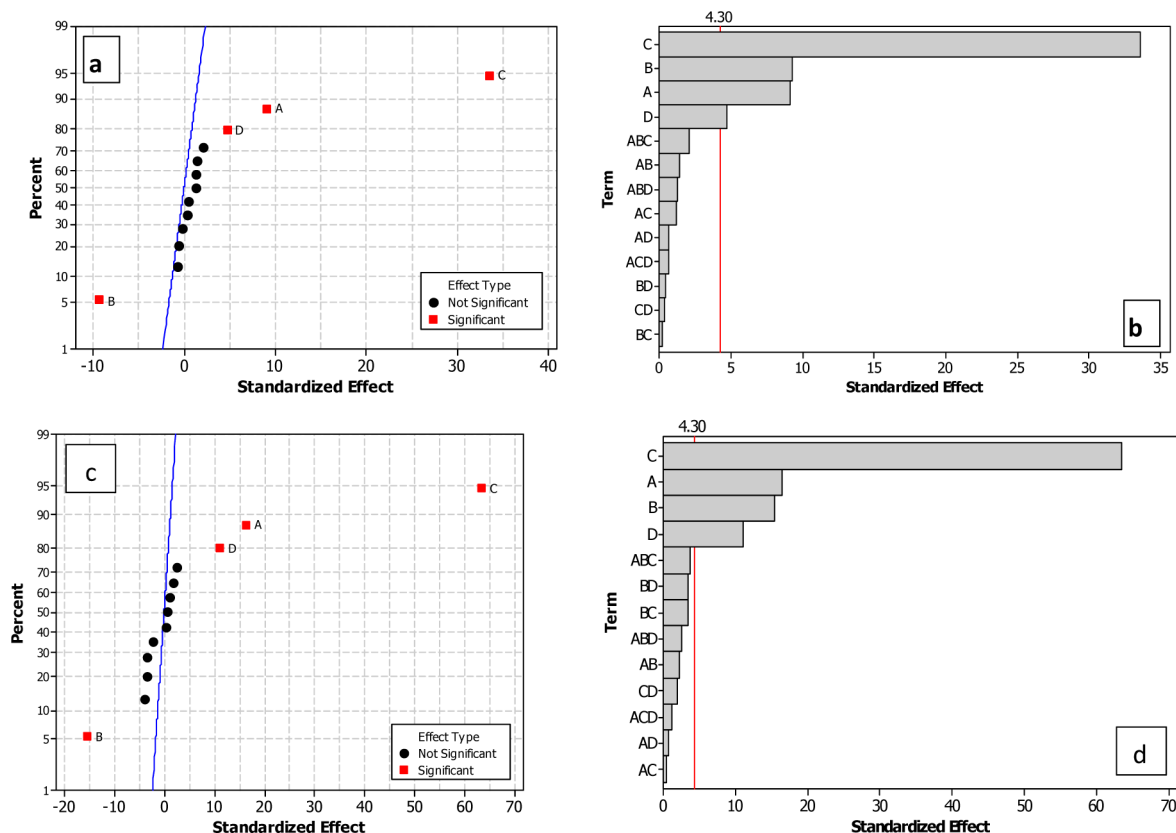


**Figure 5.** (a) Normal plot of the standardized effect of single and interaction factors on % CIP removal by MPNPs. (b) Pareto chart of the standardized effects of single and interaction factors on % CIP removal by MPNPs. (c) Normal plot of the standardized effect of single and interaction factors on % MOX removal by MPNPs. (d) Pareto chart of the standardized effects of single and interaction factors on % MOX removal by MPNPs. (A = NPs loading, B = Drug concentration, C = pH, and D = contact time).

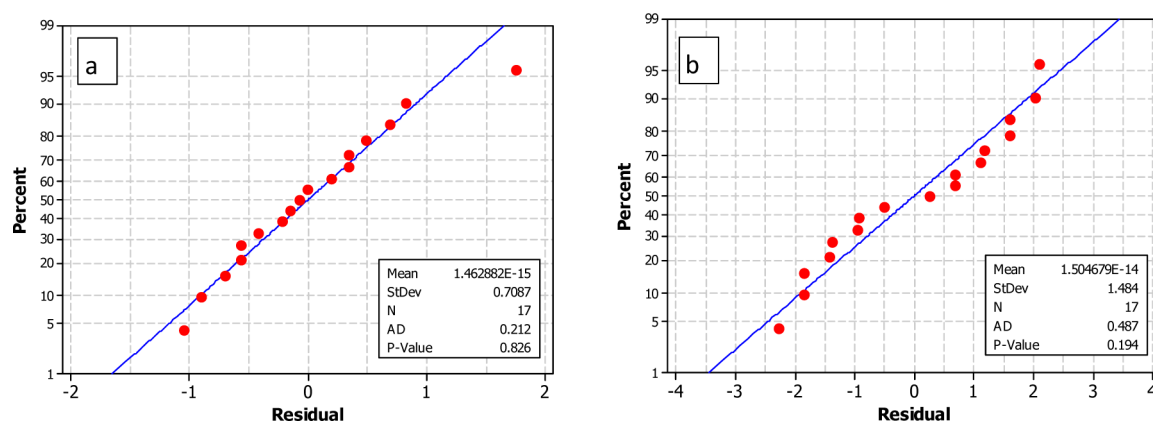


**Figure 6.** Normal probability plot of residuals for (a) CIP drug and (b) MOX drug, after adsorption on MSPNPs.

isotherms. Experiments were carried out at room temperature (25 °C) and pH 7.0. Three models were used to analyze the equilibrium adsorption data: Langmuir,<sup>42</sup> Freundlich,<sup>43</sup> and Sips.<sup>44</sup> Determination of the ideal isotherm to fit the data is based on calculation of linear regression and the values of correlation coefficients ( $R^2$ ).<sup>37</sup> The Langmuir isotherm presumes that the adsorption occurs in a monolayer form on a surface containing a limited number of identical adsorption sites.<sup>42,43</sup> The linear form of the Langmuir isotherm equation is presented in eq 1.

$$\frac{C_e}{q_e} = \frac{1}{bQ_0} + \frac{C_e}{Q_0} \quad (1)$$

where  $C_e$  is the drug concentration at equilibrium (mg/mL),  $q_e$  is the amount of drug adsorbed at equilibrium per mass of adsorbent (mg/g),  $b$  is the Langmuir equilibrium constant (mL/mg) that expresses the adsorption energy, and  $Q_0$  is the maximum adsorption capacity (mg/g).

The values of  $Q_0$  and  $b$  are calculated from the slope and intercept of the plot of  $C_e/q_e$  vs  $C_e$  for MSPNPs and MPNPs (Figure 8).

The Freundlich isotherm presumes that the surface of the adsorbent has heterogeneous surface energies, where the surface coverage affects the value of  $b$ , the energy term in the Langmuir equation.<sup>37,43</sup> The linearized form of the Freundlich adsorption isotherm equation<sup>45</sup> is



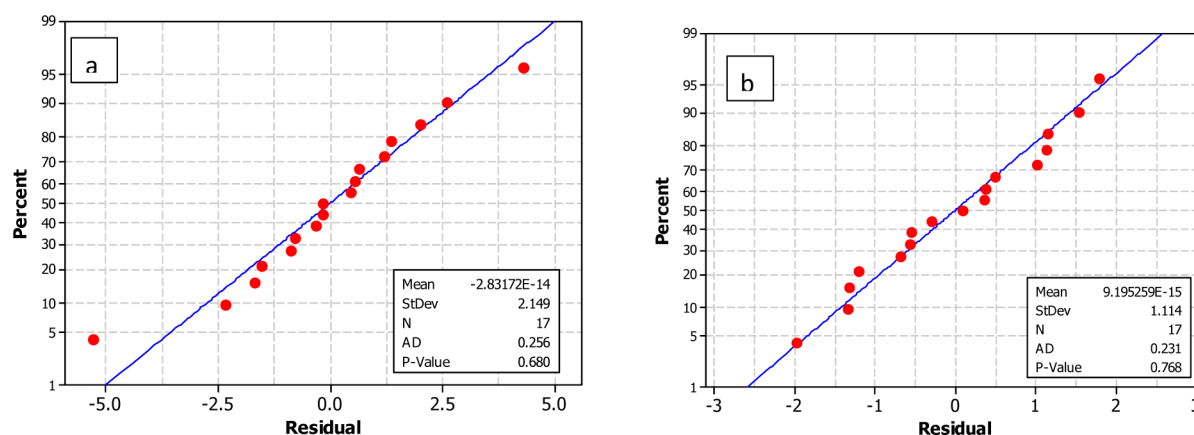


Figure 7. Normal probability plot of residuals for (a) CIP drug and (b) MOX drug, after adsorption on MPNPs.

Table 6. Regression Equations Summarizing the Experimental Design for CIP and MOX Adsorption on MSPNPs and MPNPs

NPs type	Drug	Regression equation	R <sup>2</sup>	P-value (P > 0.05)
<b>MSPNPs</b>				
	CIP	$Y = -13.8 + 7.1A - 1.52B + 14.7C + 0.201D + 0.25AB - 0.83AC - 0.009AD - 0.260BC + 0.0031BD + 0.0039CD + 0.223ABC$	0.999	0.826
	MOX	$Y = -42.5 + 49.8A + 1.97B + 18.0C + 0.405D - 4.71AB - 7.15AC + 0.175AD - 0.909BC - 0.0053BD - 0.0074CD + 1.10ABC$	0.997	0.194
<b>MPNPs</b>				
	CIP	$Y = -42.2 + 41.1A + 1.81B + 15.4C + 0.853D - 3.22AB - 5.36AC - 0.174AD - 0.833BC - 0.0205BD - 0.0267CD + 0.908ABC$	0.989	0.68
	MOX	$Y = -4.2 - 11.3A - 2.37B + 5.27C + 0.638D + 3.80AB + 7.71AC + 0.121AD + 0.518BC - 0.0610BD + 0.0421CD - 0.987ABC$	0.998	0.768

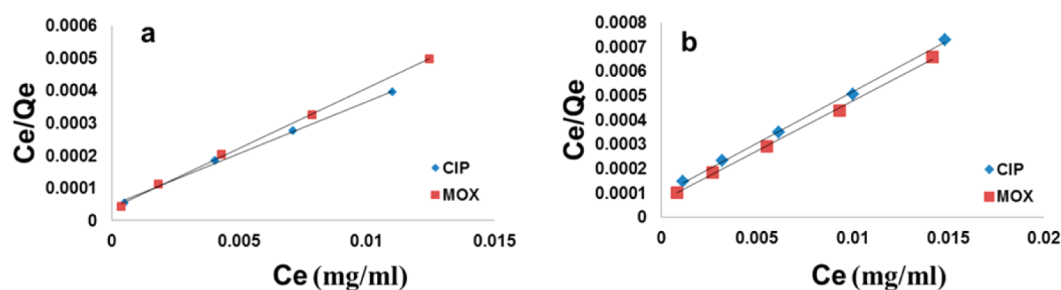


Figure 8. Fitting of isotherm data to the Langmuir model for (a) MSPNPs and (b) MPNPs. Adsorbent: 1  $\mu\text{g}/\text{mL}$ , drugs: 5–25 mg/L, temperature: 25  $^{\circ}\text{C}$ , pH: 7.0, time: 30 min.

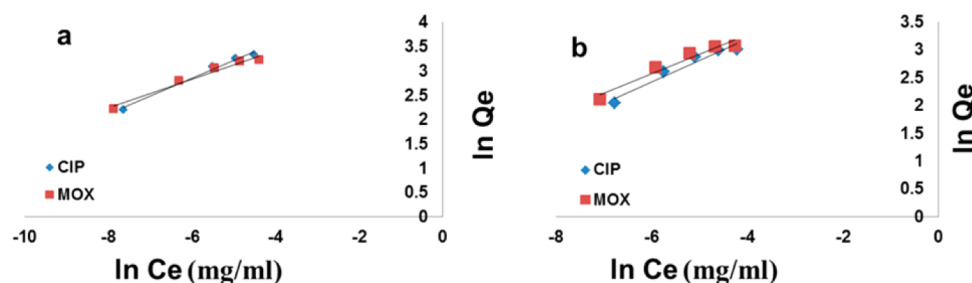
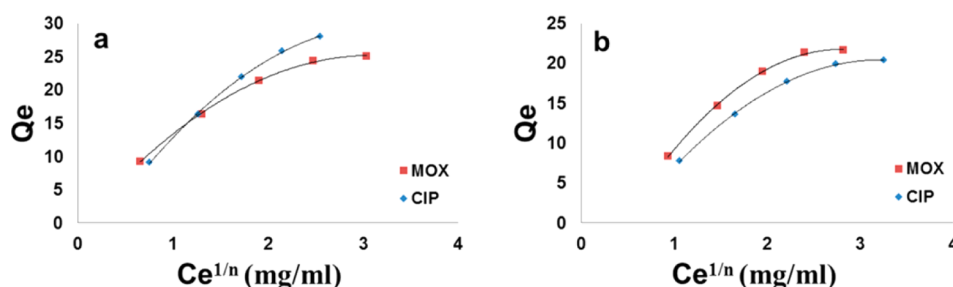


Figure 9. Fitting of isotherm data to the Freundlich model for (a) MSPNPs and (b) MPNPs. Adsorbent: 1  $\mu\text{g}/\text{mL}$ , drugs: 5–25 mg/L, temperature: 25  $^{\circ}\text{C}$ , pH: 7.0, time: 30 min.

$$\ln q_e = \ln K_f + \left(\frac{1}{n}\right) \ln C_e \quad (2)$$

where  $C_e$  is the drug concentration at equilibrium (mg/mL),  $q_e$  is the amount of drug adsorbed at equilibrium per mass of adsorbent (mg/g), and  $K_f$  ( $\text{mg}^{1-1/n} \text{ mL}^{1/n} \text{ g}^{-1}$ ) and  $1/n$  are

Freundlich constants depending on the temperature and the given adsorbent–adsorbate couple,  $n$  is related to the adsorption energy distribution, and  $K_f$  indicates the adsorption capacity. The values of  $K_f$  (mL/g) and  $1/n$  are calculated from the intercept and slope of the plot of  $\ln q_e$  vs  $\ln C_e$  for MSPNPs and MPNPs (Figure 9).



**Figure 10.** Fitting of isotherm data to the Sips model for (a) MSPNPs and (b) MPNPs. Adsorbent: 1  $\mu\text{g/mL}$ , drugs: 5–25  $\text{mg/L}$ , temperature: 25  $^{\circ}\text{C}$ , pH: 7.0, time: 30 min.

**Table 7.** Adsorption Isotherm Parameters Calculated by Langmuir, Freundlich, and Sips Equations for MSP and MPNPs

	Langmuir				Freundlich			Sips			
	$Q_0$ (mg/g)	B (mL/mg)	$R_L$	$R^2$	$K_f$ (mL/g)	$1/n$	$R^2$	$Q_m$ (mg/g)	$K_s$ (mL/mg)	$1/n$	$R^2$
MSPNPs											
CIP	31.55	634.00	0.061	0.9972	157.70	0.368	0.9836	29.91	0.41	0.389	0.9996
MOX	28.57	875.00	0.043	0.9986	100.30	0.296	0.9730	31.72	0.40	0.440	0.9997
MPNPs											
CIP	23.76	467.70	0.08	0.9983	115.78	0.387	0.9462	24.67	0.30	0.437	0.9995
MOX	24.32	587.28	0.06	0.9988	105.88	0.348	0.9477	27.27	0.34	0.391	0.9991

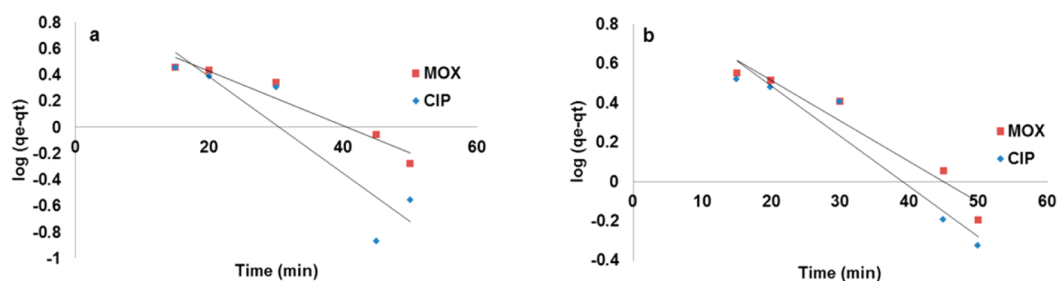


**Figure 11.** Fitting of kinetic data to pseudo-first order kinetic model for; [a] MSPNPs and [b] MPNPs. Adsorbent: 0.5  $\mu\text{g/mL}$ , Drugs 10  $\text{mg/L}$ , Temperature: 25 $^{\circ}\text{C}$ , pH: 7.0, Time: 60 min.

A more developed model was applied by Sips which is a combination of Freundlich and Langmuir equations.<sup>46</sup> Such a new isotherm model assumes that the amount of adsorbed drug increases with the increase in initial concentration, but such an increase has a finite limit, especially at high concentration of the drug.<sup>47,48</sup> The Sips<sup>44</sup> equation can be described as follows;

$$q_e = \frac{Q_m K_s C_e^{1/n}}{1 + K_s C_e^{1/n}} \quad (3)$$

where  $Q_m$  is the maximum adsorption capacity (mg/g),  $K_s$  is the Sips constant (mL/mg), and  $n$  is the Sips model exponent.

Figure 10 shows the plot of  $q_e$  vs  $C_e^{1/n}$  for MSPNPs and MPNPs, which represents the Sips isotherm curves of the studied FQs.

The calculated parameters of the studied adsorption isotherms are described in Table 7 for MSP and MPNPs. Based on the calculated correlation coefficient ( $R^2$ ) for the fitting of data to the studied isotherms, it can be concluded that Sips is the best isotherm to represent the FQs adsorption on both MSP and MPNPs. Furthermore, it was indicated from the values of  $1/n$  for the Sips isotherm that the adsorption of model FQs on the surface of MSP and MPNPs is favorable ( $0 < 1/n < 1$ ).<sup>32</sup>

The Sips isotherm equation was used to calculate the maximum adsorption capacity ( $Q_m$ ) for the model FQs at optimum pH ( $\sim 7$ ) for MSP and MPNPs, and they were estimated to be

(CIP = 29.91 mg/g, MOX = 31.72 mg/g) and (CIP = 24.67 mg/g, MOX = 27.27 mg/g), respectively. It can be noted that the values of  $Q_m$  are small, and this can be attributed to the small range of initial drug concentrations that we are working on in the present study.

**Kinetics of adsorption.** To determine the controlling mechanism for adsorption, adsorption kinetic models are usually studied. The most commonly used kinetic models are the pseudo-first-order and pseudo-second-order models.<sup>49,50</sup> The pseudo-first-order kinetic model of Lagergren<sup>51</sup> is presented by the equation:

$$\log(q_1 - q_t) = \log q_e - \frac{K_1 t}{2.303} \quad (4)$$

where  $q_t$  is the amount of drug adsorbed per unit of adsorbent (mg/g) at time  $t$ , and  $K_1$  is the pseudo-first-order rate constant ( $\text{min}^{-1}$ ). The adsorption rate constant ( $K_1$ ) was calculated from the plot of  $\log(q_e - q_t)$  against  $t$ .

While Ho and McKay<sup>52</sup> presented the pseudo-second-order kinetic as

$$\frac{t}{q_t} = \frac{1}{K_2 q_e^2} + \frac{t}{q_e} \quad (5)$$

where  $K_2$  is the pseudo-second-order rate constant ( $\text{g mg}^{-1} \text{min}^{-1}$ ). The  $q_e$  and  $K_2$  can be obtained by a linear plot of  $t/q_t$  versus  $t$ .

**Table 8. Parameters of Pseudo-First-Order and Pseudo-Second-Order Kinetic Models for the Adsorption of CIP and MOX by MSP and MPNPs**

	$q_e$ (exp) (mg/g)	Pseudo-first-order				Pseudo-second-order					
		Slope	intercept	$q_e$ (cal) (mg/g)	$K_1$ (min <sup>-1</sup> )	R <sup>2</sup>	slope	intercept	$q_e$ (cal) (mg/g)	$K_2$ (mg/g·min)	R <sup>2</sup>
<b>MSPNPs</b>											
MOX	15.688	-0.0206	0.9258	8.43	0.047	<b>0.9391</b>	0.0571	0.4669	17.513	0.0069	0.9950
CIP	17.152	-0.0256	0.9978	9.949	0.058	<b>0.9345</b>	0.0527	0.3628	18.975	0.0077	0.9960
<b>MPNPs</b>											
MOX	14.428	-0.0208	0.8427	6.961	0.0479	<b>0.9330</b>	0.0631	0.4408	15.848	0.009	0.9955
CIP	12.688	-0.0369	1.1232	13.28	0.0849	<b>0.8427</b>	0.0693	0.5641	14.43	0.0085	0.9942

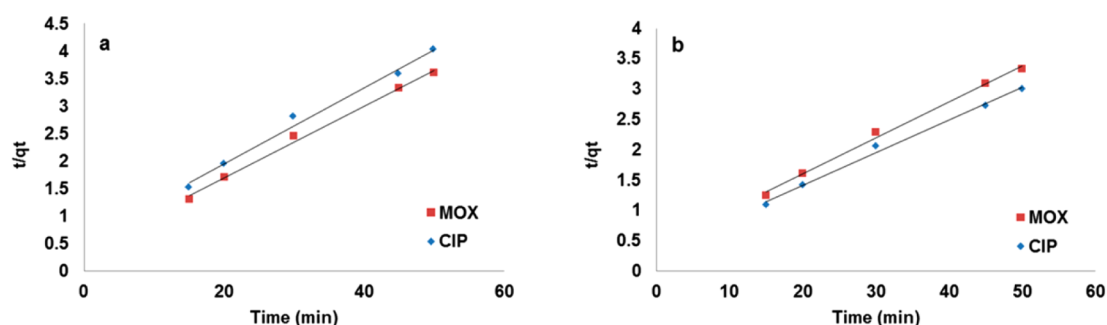
**Figure 12.** Fitting of kinetic data to a pseudo-second-order kinetic model for (a) MSPNPs and (b) MPNPs. Adsorbent: 0.5  $\mu\text{g/mL}$ , drugs: 10 mg/L, temperature: 25  $^{\circ}\text{C}$ , pH: 7.0, time: 60 min.

Figure 11(a) and (b) demonstrate the plots of the pseudo-first-order kinetics of CIP and MOX adsorption together with their photodegraded molecules on MSP and MPNPs, respectively.

The calculated kinetic parameters are presented in Table 8 for MSPNPs and MPNPs, respectively. Noticeably, the calculated  $q_e$  values ( $q_e$ , cal) obtained from the pseudo-first-order equation are not a good match to that of experimental data ( $q_e$ , exp). In addition, the values of correlation coefficient for the pseudo-first-order model were quite low. Such results indicate that the pseudo-first-order equation is not well representing the model of FQs adsorption on MSP and MPNPs.

The plots of pseudo-second-order kinetics of CIP and MOX adsorption together with their photodegraded molecules on MSP and MPNPs are presented in Figure 12(a) and (b), respectively. As indicated in Table 8, the values of calculated  $q_e$  by the pseudo-second-order equation showed a good agreement with the experimental data values with a relatively high  $R^2 \geq 0.99$ . Thus, the best fit of the data is to pseudo-second-order kinetics, and this shows that the adsorption process depends on the properties of both the model FQs and MSP and MPNPs.

## CONCLUSION

This study elaborated on the efficiency of pectin modified magnetic nanoparticles to remove FQs and their photodegraded molecules from aqueous solution. Full  $2^4$  factorial design was executed to determine the significance and interactions of factors such as pH, initial FQs concentration, NPs loading, and contact time. Statistical analysis confirmed that the adsorption of CIP and MOX together with their photodegraded molecules was enhanced by increasing the pH, NPs loading, and contact time while decreasing the initial drug concentration. ANOVA results demonstrated that the most significant factor for the model FQs adsorption was pH, where the adsorption was dependent on the electrostatic force of attraction between the drugs and the adsorbents upon pH adjustment. Concentration analysis was done using a validated spectrofluorimetric method. Adsorption

kinetics was fitted with the pseudo-second-order model, and adsorption isotherms were best described by the Sips equation. In conclusion, MSPNPs and MPNPs could be used as an efficient and promising adsorbent to remove FQs together with their photodegraded molecules from aqueous solution, and in future work, it can be a test to remove other drugs and their degradates from wastewater.

## ASSOCIATED CONTENT

### Supporting Information

The Supporting Information is available free of charge on the ACS Publications website at DOI: 10.1021/acssuschemeng.6b01003.

Analysis of variance for removal of CIP and MOX using MSP NPs; and interaction effect plots of MSPNPs for the removal efficiency (%) on CIP and MOX (PDF)

## AUTHOR INFORMATION

### Corresponding Author

\*E-mail: marianne.morcos@pharma.cu.edu.eg

### ORCID

Medhat A. Al-Ghobashy: 0000-0002-3270-6804

Marianne Nebsen: 0000-0002-0687-2358

### Notes

The authors declare no competing financial interest.

## REFERENCES

- Peterson, J. W.; Gu, B.; Seymour, M. D. Surface interactions and degradation of a fluoroquinolone antibiotic in the dark in aqueous TiO<sub>2</sub> suspensions. *Sci. Total Environ.* **2015**, 532, 398–403.
- Gupta, K. C.; Devi, S. G. Photo and UV degradation of Ciprofloxacin Antibiotic. *Int. J. Curr. Microbiol. Appl. Sci.* **2014**, 3 (6), 641–648.
- Hubicka, U.; Zmudzki, P.; Talik, P.; Zuromska-Witek, B.; Krzek, J. Photodegradation assessment of ciprofloxacin, moxifloxacin, norflox-

acin and ofloxacin in the presence of excipients from tablets by UPLC-MS/MS and DSC. *Chem. Cent. J.* **2013**, *7*, 133.

(4) Yao, H.; Lu, J.; Wu, J.; Lu, Z.; Wilson, P. C.; Shen, Y. Adsorption of Fluoroquinolone Antibiotics by Wastewater Sludge Biochar: Role of the Sludge Source. *Water, Air, Soil Pollut.* **2013**, *224* (1), 1370.

(5) Hu, J.; Wang, W.; Zhu, Z.; Chang, H.; Pan, F.; Lin, B. Quantitative Structure–Activity Relationship Model for Prediction of Genotoxic Potential for Quinolone Antibacterials. *Environ. Sci. Technol.* **2007**, *41* (13), 4806–4812.

(6) Wei, H.; Hu, D.; Su, J.; Li, K. Intensification of levofloxacin sonodegradation in a US/H<sub>2</sub>O<sub>2</sub> system with Fe<sub>3</sub>O<sub>4</sub> magnetic nanoparticles. *Chin. J. Chem. Eng.* **2015**, *23* (1), 296–302.

(7) Le-Minh, N.; Khan, S. J.; Drewes, J. E.; Stuetz, R. M. Fate of antibiotics during municipal water recycling treatment processes. *Water Res.* **2010**, *44* (15), 4295–4323.

(8) López-Serna, R.; Pérez, S.; Ginebreda, A.; Petrović, M.; Barceló, D. Fully automated determination of 74 pharmaceuticals in environmental and waste waters by online solid phase extraction-liquid chromatography-electrospray-tandem mass spectrometry. *Talanta* **2010**, *83* (2), 410–424.

(9) Paul, T.; Dodd, M. C.; Strathmann, T. J. Photolytic and photocatalytic decomposition of aqueous ciprofloxacin: Transformation products and residual antibacterial activity. *Water Res.* **2010**, *44* (10), 3121–3132.

(10) An, T.; Yang, H.; Song, W.; Li, G.; Luo, H.; Cooper, W. J. Mechanistic considerations for the advanced oxidation treatment of fluoroquinolone pharmaceutical compounds using TiO<sub>2</sub> heterogeneous catalysis. *J. Phys. Chem. A* **2010**, *114* (7), 2569–2575.

(11) Xing, X.; Feng, J.; Lv, G.; et al. Adsorption Mechanism of Ciprofloxacin from Water by Synthesized Birnessite. *Adv. Mater. Sci. Eng.* **2015**, *2015*, 1–7.

(12) Challis, J. K.; Hanson, M. L.; Friesen, K. J.; Wong, C. S. A critical assessment of the photodegradation of pharmaceuticals in aquatic environments: defining our current understanding and identifying knowledge gaps. *Environ. Sci. Process Impacts.* **2014**, *16* (4), 672–696.

(13) Advanced Oxidation Processes. Neopure Technologies. Available at: <http://neopuretech.com/advanced-oxidation-processes/> at 2 April 2016.

(14) Saleh, S. M. HPLC Determination of Four Textile Dyes and Studying Their Degradation Using Spectrophotometric Technique. M.Sc. thesis, Chemistry department, An-Najah National University, Palestine, 2005.

(15) Sivashankar, R.; Sathya, A. B.; Vasantharaj, K.; Sivasubramanian, V. Magnetic composite an environmental super adsorbent for dye sequestration – A review. *Environ. Nanotechnology, Monit Manag.* **2014**, *1* (2), 36–49.

(16) Shu, J.; Wang, Z.; Huang, Y.; Huang, N.; Ren, C.; Zhang, W. Adsorption removal of Congo red from aqueous solution by polyhedral Cu<sub>2</sub>O nanoparticles: Kinetics, isotherms, thermodynamics and mechanism analysis. *J. Alloys Compd.* **2015**, *633*, 338–346.

(17) Huang, X.; Wang, Y.; Liu, Y.; Yuan, D. Preparation of magnetic poly(vinylimidazole-co-divinylbenzene) nanoparticles and their application in the trace analysis of fluoroquinolones in environmental water samples. *J. Sep. Sci.* **2013**, *36* (19), 3210–3219.

(18) Zheng, H.-B.; Mo, J.-Z.; Zhang, Y.; et al. Facile synthesis of magnetic molecularly imprinted polymers and its application in magnetic solid phase extraction for fluoroquinolones in milk samples. *J. Chromatogr. A* **2014**, *1329*, 17–23.

(19) Xiao, D.; Dramou, P.; Xiong, N.; et al. Preparation of molecularly imprinted polymers on the surface of magnetic carbon nanotubes with a pseudo template for rapid simultaneous extraction of four fluoroquinolones in egg samples. *Analyst* **2013**, *138* (11), 3287–3296.

(20) Wang, Z.; Chen, M.; Shu, J.; Li, Y. One-step solvothermal synthesis of Fe<sub>3</sub>O<sub>4</sub>@Cu@Cu<sub>2</sub>O nanocomposite as magnetically recyclable mimetic peroxidase. *J. Alloys Compd.* **2016**, *682*, 432–440.

(21) Lin, Y.; Weng, C.; Chen, F. Effective removal of AB24 dye by nano/micro-size zero-valent iron. *Sep. Purif. Technol.* **2008**, *64* (1), 26–30.

(22) Madhav, A. Evaluation of fruit wastes as sources of pectin. M.Sc. (Hott) thesis, Kerala Agricultural University, Thrissur, India, 2001.

(23) GITCO. Gujarat Industrial and Technical Consultancy Organization Limited, GITCO House, Ahmadabad, Twenty-five Prospective Food Processing Projects 2:52. 1999. <http://www.gujagro.org/pdf/guidelines.pdf>. Accessed September 27, 2015.

(24) Liming, D.; Qingqin, X.; Jianmei, Y. Fluorescence spectroscopy determination of fluoroquinolones by charge-transfer reaction. *J. Pharm. Biomed. Anal.* **2003**, *33* (4), 693–698.

(25) Xuan, C. S.; Wang, Z. Y.; Song, J. L. Spectrophotometric Determination of Some Antibacterial Drugs Using p-Nitrophenol. *Anal. Lett.* **1998**, *31* (7), 1185–1195.

(26) Jaber, A. M. Y.; Lounici, A. Polarographic behaviour and determination of norfloxacin in tablets. *Anal. Chim. Acta* **1994**, *291* (1–2), 53–64.

(27) Rizk, M.; Belal, F.; Ibrahim, F.; Ahmed, S.; EL-Enany, N. Voltammetric analysis of certain 4-quinolones in pharmaceuticals and biological fluids. *J. Pharm. Biomed. Anal.* **2000**, *24* (2), 211–218.

(28) Hernández, M.; Borrull, F.; Calull, M. Determination of quinolones in plasma samples by capillary electrophoresis using solid-phase extraction. *J. Chromatogr., Biomed. Appl.* **2000**, *742* (2), 255–265.

(29) Eastman, J. W. Quantitative spectrofluorimetry—the fluorescence quantum yield of quinine sulfate. *Photochem. Photobiol.* **1967**, *6* (1), 55–72.

(30) DrugBank: Ciprofloxacin; available at: <http://www.drugbank.ca/drugs/DB00537>. Accessed March 26, 2016.

(31) DrugBank: Moxifloxacin; available at <http://www.drugbank.ca/drugs/DB00218>. Accessed March 26, 2016.

(32) Attallah, O. A.; Al-Ghobashy, M. A.; Nebsen, M.; Salem, M. Y. Removal of cationic and anionic dyes from aqueous solution with magnetite/pectin and magnetite/silica/pectin hybrid nanocomposites: kinetic, isotherm and mechanism analysis. *RSC Adv.* **2016**, *6* (14), 11461–11480.

(33) Guideline I. Q2A Text on Validation of Analytical Procedures. *Fed. Regist.* **1994**. <http://www.hc-sc.gc.ca/dhp-mps/prodpharma/applic-demande/guide-ld/ich/qual/q2a-eng.php>. Accessed April 29, 2015.

(34) Guideline I. Validation of analytical procedures: Text and Methodology. Q2. **2005**. <http://somatek.com/content/uploads/2014/06/sk140605h.pdf>. Accessed April 29, 2015.

(35) International Conference on Harmonization (ICH), Q2B, *Validation of Analytical Procedures: Definitions and Terminology*, Vol. 60, US FDA Federal Register, 1995.

(36) Mater, N.; Geret, F.; Castillo, L.; Faucet-Marquis, V.; Albasi, C.; Pfohl-Leschkowicz, A. In vitro tests aiding ecological risk assessment of ciprofloxacin, tamoxifen and cyclophosphamide in range of concentrations released in hospital wastewater and surface water. *Environ. Int.* **2014**, *63*, 191–200.

(37) Ozbay, N.; Yargic, A. S. Factorial experimental design for Remazol Yellow dye sorption using apple pulp/apple pulp carbon–titanium dioxide co-sorbent. *J. Cleaner Prod.* **2015**, *100*, 333–343.

(38) Safa, Y.; Bhatti, H. N. Adsorptive removal of direct textile dyes by low cost agricultural waste: Application of factorial design analysis. *Chem. Eng. J.* **2011**, *167* (1), 35–41.

(39) Safa, Y.; Bhatti, H. N. Biosorption of Direct Red-31 and Direct Orange-26 dyes by rice husk: Application of factorial design analysis. *Chem. Eng. Res. Des.* **2011**, *89* (12), 2566–2574.

(40) Nadim, A. H.; Al-Ghobashy, M. A.; Nebsen, M.; Shehata, M. A. Gallic acid magnetic nanoparticles for photocatalytic degradation of meloxicam: synthesis, characterization and application to pharmaceutical wastewater treatment. *RSC Adv.* **2015**, *5* (127), 104981–104990.

(41) Pokhrel, D.; Viraraghavan, T. Arsenic Removal from Aqueous Solution by Iron Oxide-Coated Fungal Biomass: A Factorial Design Analysis. *Water, Air, Soil Pollut.* **2006**, *173* (1–4), 195–208.

(42) Langmuir, I. The adsorption of gases on plane surfaces of glass, mica and platinum. *J. Am. Chem. Soc.* **1918**, *40* (9), 1361–1403.

(43) Freundlich, H. *Über Die Adsorption in Lösungen*; Wilhelm Engelmann in Leipzig: 1906.

(44) Sips, R. On the Structure of a Catalyst Surface. *J. Chem. Phys.* **1948**, *16* (5), 490.

- (45) Badruddoza, A. Z. M.; Hazel, G. S. S.; Hidajat, K.; Uddin, M. S. Synthesis of carboxymethyl- $\beta$ -cyclodextrin conjugated magnetic nano-adsorbent for removal of methylene blue. *Colloids Surf, A* **2010**, *367* (1–3), 85–95.
- (46) Muntean, S. G.; Paska, O.; Coseri, S.; Simu, G. M.; Grad, M. E.; Iliu, G. Evaluation of a functionalized copolymer as adsorbent on direct dyes removal process: Kinetics and equilibrium studies. *J. Appl. Polym. Sci.* **2013**, *127* (6), 4409–4421.
- (47) Paşka, O. M.; Păcurariu, C.; Muntean, S. G. Kinetic and thermodynamic studies on methylene blue biosorption using corn-husk. *RSC Adv.* **2014**, *4* (107), 62621–62630.
- (48) Lim, L. B. L.; Priyantha, N. Mansor NHM. Artocarpus altilis (breadfruit) skin as a potential low-cost biosorbent for the removal of crystal violet dye: equilibrium, thermodynamics and kinetics studies. *Environ. Earth Sci.* **2015**, *73* (7), 3239–3247.
- (49) Anirudhan, T. S.; Radhakrishnan, P. G.; Vijayan, K. Development of a First-Order Kinetics Based Model, Equilibrium Studies, and Thermodynamics for the Adsorption of Methyl Orange onto a Lignocellulosic Anion Exchanger. *Sep. Sci. Technol.* **2013**, *48* (6), 947–959.
- (50) Wang, L.; Li, J.; Wang, Y.; Zhao, L. Preparation of nanocrystalline  $\text{Fe}_{(3-x)}\text{La}_x\text{O}_4$  ferrite and their adsorption capability for Congo red. *J. Hazard. Mater.* **2011**, *196*, 342–349.
- (51) Lagergren, S. *About the Theory of so-Called Adsorption of Soluble Substances*, Kungliga Svenska Vetenskapsakademiens. Handlingar 24; 1898.
- (52) Ho, Y.; McKay, G. Pseudo-second order model for sorption processes. *Process Biochem.* **1999**, *34* (5), 451–465.